CSI Fingerprint and GCN Based Indoor Localization Using Graph Structures Fusion

Shuting Fan
College of Telecommunications and Information Engineering
Nanjing University of Posts and Telecommunications
Nanjing, China, 210003
E-mail: jshmfst@126.com

Jun Yan
College of Telecommunications and Information Engineering
Nanjing University of Posts and Telecommunications
Nanjing, China, 210003
E-mail: yanj@njupt.edu.cn

2023 IEEE 23rd International Conference on Communication Technology (ICCT) | 979-8-3503-2595-9/23/$31.00 ©2023 IEEE | DOI: 10.1109/ICCT59356.2023.10419794

***Abstract*—Since the channel state information (CSI) can provide a fine-grained description of signal propagation process, in this paper, a new CSI fingerprint and graph convolutional network (GCN) based indoor localization algorithm is proposed. First, the amplitude and phase information of CSI measurement is extracted for amplitude and phase based CSI gray image construction,respectively. And then, the corresponding CSI RGB images are obtained by the image render techniques. Next, a pixel value comparison based rule is used to form the graph structure of each channel of the amplitude and phase based CSI image. The front-end fusion is used to form the final graph structure. At last, the GCN model is used to training the graph structure.Some Experiments are carried out to verify the performance of the proposed algorithm.**

***Index Terms*—Indoor localization; Channel State Information; Front-end Fusion; Graph Convolutional Network; Deep Learning**

I. Introduction

With the development of wireless communication technology, the need for location-based services is increases. Since satellite based localization is limited in indoor environment, indoor localization technology has been received much attentions.

At present, the indoor localization measurements includes time of arrival (TOA) [1], time difference of arrival (TDOA) [2], angle of arrival (AOA) [3] and receive signal strength indicators (RSSI) [4]. Recently, channel state information (CSI) measurement [5] become a popular measurement for localization purpose. Compared with RSSI measurement, CSI provides more abundant and fine-grained information from frequency domain. The authors of [6] proposed deep convolutional neural network based CSI localization algorithm. In. [7], a Splicer system is proposed to eliminate mixed hardware errors in CSI measurement data. In [8], a positioning algorithm that integrates CSI amplitude and phase information is proposed. The combination of CSI amplitude information and phase information can indeed obtain better localization performance.

Now,with the development of machine learning, graph neural network (GNN) [9]–[11] has been used for indoor localization. The authors of [12] used the graph structure generated by Radio Frequency Identification (RFID) signals to realize indoor positioning. A GCN based localization algorithm by RSSI measurement is proposed in [13]. The authors of [14] proposed GNN based indoor localization, which the distance between APs generated edges to construct the graph structure. In [15], a Euclidian distance threshold to classify whether edges can be formed is proposed to construct graph structure for GCN based localization. The authors of [16] proposed a visual positioning system based on point cloud GNN. In [17], GNN combined with transfer learning is proposed for device-free location. The authors of [18] proposed a collaborative graph convolutional network (C-GCN) composed of convolutional layer and graph convolutional layer based on GCN.

In this paper, a new GCN based CSI indoor localization algorithm is proposed. First,the amplitude information and phase information of CSI measurement is used to generate the CSI gray image. And then the CSI gray image is convert into the RGB image through rendering technique. Then, the CSI RGB image is proposed to form the corresponding graph structure of R, G and B channels. Finally, the three-channel graph structure constructed by the amplitude information and phase information is fused into a complete graph structure for GCN training.

II. Algorithm framework structure

According to the block diagram shown Fig1, the proposed algorithm includes the following steps: (1) CSI measurement data preprocessing: after obtaining the amplitude information and phase information of CSI measurement data, the phase information is processed by linear transformation to solve the problem of excessive phase interference information. (2) CSI amplitude and phase image construction: first,the amplitude information matrix and phase information matrix is transformed into CSI gray image. Then, the gray image obtained is converted to CSI RGB color image by image rendering technology. (3) The graph structure fusion of CSI images: the amplitude or phase CSI RGB color image is constructed as a graph structure. Then, each kind of RGB CSI images are fused based on the graph structure of R,G, and B channel. At last, the fused graph structures of amplitude and phase CSI images are fused once again to form final graph structure for GCN training. and (4) Offline classification learning based on GCN.

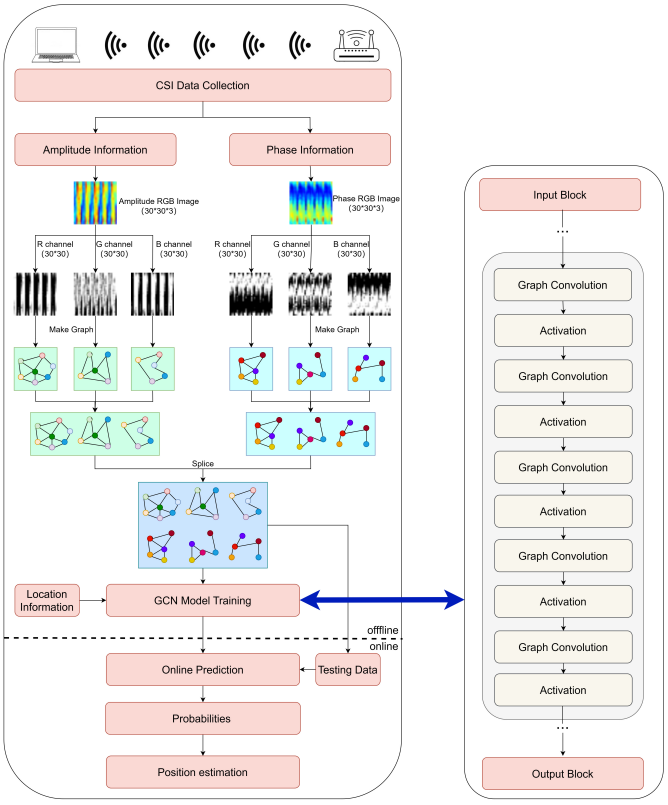

Fig. 1. Overall block diagram of the algorithm in this paper

III. Algorithm Description

A. CSI measurement data preprocessing

Since the phase information of CSI measurement may has some error, the phase linear calibration is proposed to preprocess the phase information.

Assume the phase information of the ith subcarrier after unwinding is expressed as:

$$\tilde{\theta}_i = \theta_i + \frac{2\pi K_i \Delta t}{N} + \beta + Z_f \tag{1}$$

Where θ_i is the true phase, Δt is the timing error offset, K_i is the subcarrier index, N is the number of fast Fourier transform , β is the random phase offset, and Z_f is the random measurement noise.

In order to obtain the true phase, the delay Δt and phase shift β should be eliminated. Using linear transformation method, the slope a and offset b of the phase are described as:

$$a = \frac{\tilde{\theta_n} - \tilde{\theta_1}}{K_n - K_1} \tag{2}$$

$$b = \frac{1}{n}\sum_{i=1}^{n} \tilde{\theta}_i \tag{3}$$

The real phase can be obtained by removing the linear term by:

$$\tilde{\theta}_i = \tilde{\theta}_i - aK_i - b = \tilde{\theta}_i - \frac{\tilde{\theta_n} - \tilde{\theta_1}}{K_n - K_1} K_i - \frac{1}{n}\sum_{i=1}^{n} \tilde{\theta}_i \tag{4}$$

In order to obtain the uniform distribution of the corresponding subcarriers, the subcarrier phase should be unwrapped before the linear transformation, and then the phase will be linearly transformed. Fig2 describes the result of phase calibration.

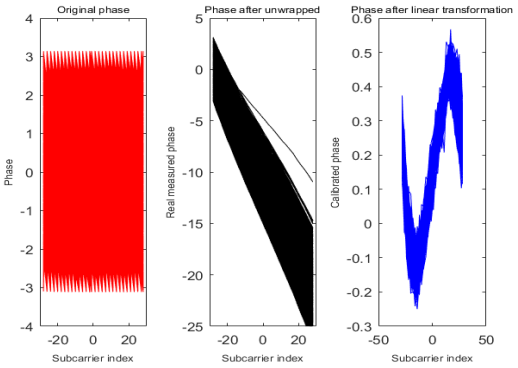

Fig. 2. The description of phase calibration results

B. CSI image construction

In this step, the CSI amplitude information and phase information are used to transform into the CSI RGB images. In the following, taking CSI amplitude information as an example, CSI amplitude image construction process is described.

Defined T_x and R_x are the number of transmitting antennas and receiving antennas, n is the number of subcarriers, and K is the number of data packets used to construct an image. First, N_c amplitude information of a subcarrier in a data packet can be described as a vector $[A_1, A_2, ..., A_{N_c}]$, where $N_c = T_x * R_x$. The amplitude information of all subcarrier can be described as:

$$H_A = \begin{bmatrix} A_{1,1} & A_{1,2} & \cdots & A_{1,N_c} \\ A_{2,1} & A_{2,2} & \cdots & A_{2,N_c} \\ \vdots & \vdots & \ddots & \vdots \\ A_{n,1} & A_{n,2} & \cdots & A_{n,N_c} \end{bmatrix} \tag{5}$$

In this paper, the size of the CSI image is set as $n*n$. Due to $N_c < n$, CSI amplitude information of K data packets is required to form an $n*n$ dimensional matrix, where $K*N_c = n$. And then, the element data of amplitude information in the matrix is mapped to the range of 0-255 to form the gray image. At last, the obtained CSI gray image is converted into the CSI RGB image by image rendering technology.

Fig3(a) and Fig3(b) describe amplitude based CSI RGB images at different positions. While, Fig3(c) and Fig3(d) describe phase based CSI RGB images at different positions. From the figures, we can found that the proposed CSI RGB image construction method can be used for classification learning, since the images of different positions are different.

C. Graph structure construction of CSI images

In this step, the amplitude and phase based CSI RGB images are converted into the graph structure.

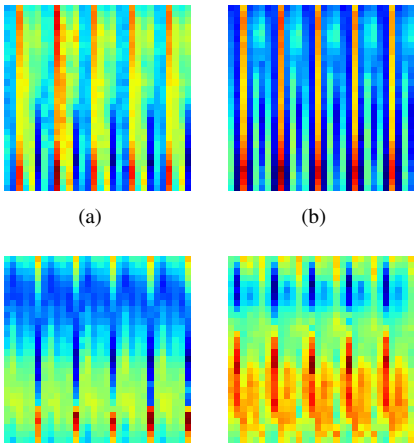

(a) (b) (c) (d)

Fig. 3. The description of CSI RGB images when the target located at different reference points

The RGB color images can divide into R,G and B channels. For the images in channels R, G and B, the graph structure construction is shown in Fig4. Taking the image of one channel with size of 3∗3 as an example, by the given threshold,the pixel value larger than the threshold is chosen as a node to construct the graph structure. Assume that the threshold number is 150. As shown on the left of Fig4, the image will have 5 nodes. Looking for 8 pixels around every node, if they are all nodes, they will be connected to each other. In this way, the graph structure shown on the right of Fig4 can be obtained.

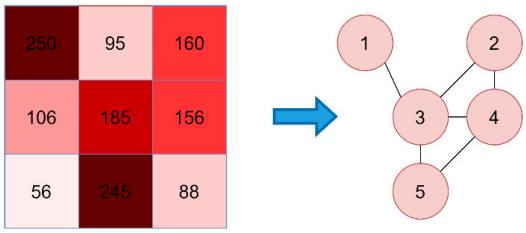

Fig. 4. The schematic diagram of structure construction

According to Eq. 6, the adjacency matrix can be obtained by Eq. 7.

$$A_{i,j} = \begin{cases} 1, where\ node\ i\ is\ connected\ to\ node\ j \\ 0, where\ node\ i\ is\ not\ connected\ to\ node\ j \end{cases} \tag{6}$$

$$A = \begin{bmatrix} 0 & 0 & 1 & 0 & 0 \\ 0 & 0 & 1 & 1 & 0 \\ 1 & 1 & 0 & 1 & 1 \\ 0 & 1 & 1 & 0 & 1 \\ 0 & 0 & 1 & 1 & 0 \end{bmatrix} \tag{7}$$

Where, the ith row and the jth column of the adjacency matrix A indicates whether the ith node and the jth node are connected.

Next, choosing the coordinate of the current pixel as the node feature, the feature matrix of the graph structure in the right of Fig4 can be described as:

$$\begin{bmatrix} 1 & 1 \\ 1 & 3 \\ 2 & 2 \\ 2 & 3 \\ 3 & 2 \end{bmatrix} \tag{8}$$

According to Fig5, after constructing the graph structure of R, G and B channels of amplitude and phase based CSI RGB image, the graph structures are fusion to form the final graph structure.

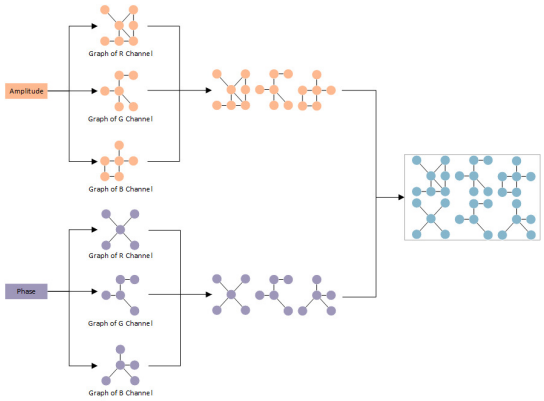

Fig. 5. The fusion of graph structure

D. Offline classification learning based on GCN

The structure of the graph convolutional network in this paper is shown in Fig6. It contains 5 layers of graph convolution layer (GCN), 5 activation functions (ReLu), 2 layers of full connection layer (FC) and an output layer (Output).

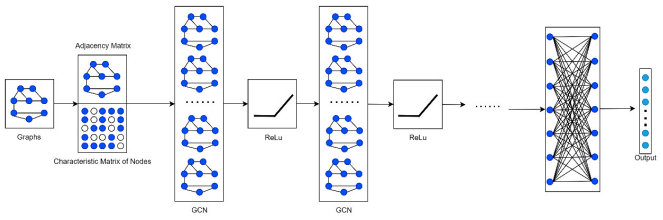

Fig. 6. Convolutional Neural network structure diagram

The graph structure (adjacency matrix, node characteristic matrix) and corresponding position label are chosen input for the graph convolutional neural network to learn the relationship between the graph structure and position label.

Then, the features extracted by 5 layers convolutional layer (GCN) and 5 activation functions (ReLu) are input to the classification layer. In this paper, two fully connected layers (FC) are selected to realize the final classification as shown in Fig.7. The fully connected layer is realized by:

$$y = f(Wx + \beta) \tag{9}$$

Where, y is the output of the fully connected layer of each layer. $f(x)$ is the ReLU activation function. W represents the weight matrix of the fully connected layer. x is the input of the full connection layer; β is biased.

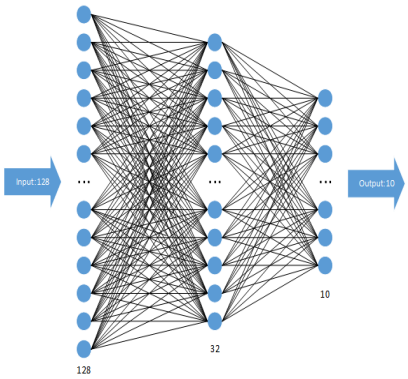

Fig. 7. Schematic diagram of the fully connected layer

In the two fully connected layers, the parameter of the first and second fully connected layer are 128*32 and 32*10 respectively.The final result will be obtained by the output layer.

IV. Experimental Analysis

A. Experimental Scenarios

The experimental environment is selected on the 20th floor of the Scientific Research Building of NJUPT. Fig.8(a) is the actual experimental scene. Fig. 8(b) is the layout of the experimental environment. The first reference point, namely L1, is taken as coordinate $(0, 0)$, and each reference point is 60cm apart. At each reference point, 400 CSI amplitude information images and 400 CSI phase information images are obtained.

(a) The actual experimental scene

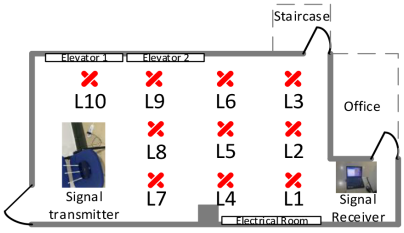

(b) Experiment layout

Fig. 8. The description of experimental scene

In the experiment, Lenovo computer with Intel 5300AGN wireless network card is chosen as the receiver with three antennas. A three-antenna TP-LINK router is chosen as a transmitter. For CSI measurement collection,the parameters of computer are given by Intel Core i7-4770 CPU , 8GB memory. The operating system is Ubuntu 14.04. The CSI-Tool software tool also is installed. The training environment in this experiment is Intel Core i7-7700HQ with 8G memory. The operating system is Windows10, the language is Python3.9 and the deep learning framework uses Pytorch.

B. Performance Description

Fig9 describes the localization performance of the proposed algorithm under different training epochs. From the figure, when the training epochs continue to increase, the loss tends to converge and the accuracy also increases. When the number of epoch is 2000, the accuracy can reach 96.75%.

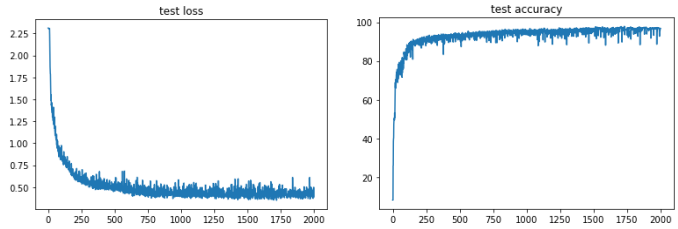

Fig. 9. Positioning performance of the proposed algorithm under different training epochs

Table I shows Recall, Precision, and F1 score, weighted harmonic average index of Precision and Recall, at different locations. According to the data in the table, it can be seen that the proposed algorithm is perform well.

TABLE I
Recall, Precision and F1 score of different positions

Location	**L1**	**L2**	**L3**	**L4**	**L5**
Recall	0.9720	0.9823	0.9636	0.9737	0.9509
Precision	0.9522	0.9703	0.9761	0.9715	0.9672
F1 score	0.9620	0.9763	0.9698	0.9726	0.9590
Location	**L6**	**L7**	**L8**	**L9**	**L10**
Recall	0.9678	0.9943	0.9828	0.9525	0.9159
Precision	0.9546	0.9707	0.9758	0.9673	0.9659
F1 score	0.9612	0.9824	0.9793	0.9598	0.9402

Table II shows the localization performance of the proposed algorithm under different number of training data. According to the data in the table, when the number of training data increases, the accuracy of the proposed algorithm also increases. However, Mean Absolute Error (MAE), Mean Square Error (MSE) and Root Mean Square Error (RMSE) all decrease which describe better position estimation result.

C. Performance Comparison

First, amplitude-only information and phase-only information are chosen for performance comparison. As shown in Table III, the MAE, MSE and RMSE and the accuracy are

TABLE II
PERFORMANCE DESCRIPTION UNDER DIFFERENT NUMBER OF TRAINING DATA

Different numbers	MAE	MSE	RMSE	Acc
400	0.639	2.610	1.616	81.44%
800	0.615	2.377	1.542	82.62%
1200	0.468	1.848	1.359	84.53%
1600	0.339	1.316	1.147	88.11%
2000	0.309	1.265	1.125	92.20%
2400	0.271	1.085	1.042	94.19%
2800	0.267	1.019	1.009	96.08%
3200	0.263	1.005	1.002	96.75%

compared. The accuracy of the proposed algorithm can finally reach 96.75%, while the accuracy of amplitude-only information can reach 94.50%, and that of phase-only information can only reach 82.75%. Therefore, the proposed algorithm has some advantages for accurate position estimation. Moreover, the MAE, MSE and RMSE of the proposed algorithm is also minimal. Thus, the proposed algorithm can achieve best localization results amomg the above approaches.

TABLE III
LOCALIZATION PERFORMANCE COMPARISON OF THE PROPOSED ALGORITHM, AMPLITUDE-ONLY INFORMATION AND PHASE-ONLY INFORMATION UNDER DIFFERENT NUMBER OF TRAINING DATA

		Acc	MAE	MSE	RMSE
amplitude-only information	**1200**	77.14%	0.538	1.994	1.412
	1600	85.88%	0.362	1.354	1.164
	2000	90.62%	0.295	1.158	1.076
	2400	91.90%	0.294	1.124	1.060
	2800	93.83%	0.280	1.112	1.055
	3200	94.50%	0.272	1.028	1.014
phase-only information	**1200**	69.29%	1.052	5.366	2.317
	1600	75.75%	0.923	4.891	2.212
	2000	78.85%	0.770	3.889	1.972
	2400	79.12%	0.739	3.714	1.927
	2800	81.75%	0.709	3.703	1.924
	3200	82.75%	0.690	3.541	1.882
the proposed algorithm	**1200**	84.53%	0.468	1.848	1.359
	1600	88.11%	0.339	1.316	1.147
	2000	92.20%	0.309	1.265	1.125
	2400	94.19%	0.271	1.085	1.042
	2800	96.08%	0.267	1.019	1.009
	3200	96.75%	0.263	1.005	1.002

Second, the front end fusion based on Generative adversarial network(GAN) is chosen for comparison. According to the results shown in Table IV, compared with the front-end fusion algorithm based on GAN, the proposed algorithm has better results both in accuracy and localization error.

Third, when the number of training data is 3200, the proposed algorithm compared the algorithms based on back-end fusion and mid-layer feature fusion. As shown in Table V, the proposed algorithm perform better than the feature fusion of the middle layer and the algorithm based on back-end fusion. In addition, in the training process, due to the fact that the training time of the algorithm based on the feature fusion of the middle layer is about three times that of the proposed algorithm, while the training time of the algorithm based on back-end fusion is more than twice that of the proposed algorithm, the time of the proposed algorithm is much lower

TABLE IV
COMPARISON OF POSITIONING PERFORMANCE BASED ON DIFFERENT FRONT-END FUSION ALGORITHMS UNDER DIFFERENT TRAINING SAMPLES

		Acc	MAE	MSE	RMSE
front-end fusion based on GAN	**1200**	70.30%	1.088	4.340	2.083
	1600	82.39%	0.556	2.260	1.503
	2000	84.71%	0.552	2.170	1.473
	2400	85.62%	0.522	2.018	1.421
	2800	88.17%	0.431	1.739	1.319
	3200	90.25%	0.346	1.386	1.177
the proposed algorithm	**1200**	84.53%	0.468	1.848	1.359
	1600	88.11%	0.339	1.316	1.147
	2000	92.20%	0.309	1.265	1.125
	2400	94.19%	0.271	1.085	1.042
	2800	96.08%	0.267	1.019	1.009
	3200	96.75%	0.263	1.005	1.002

than that of the other two algorithms. Therefore, the proposed algorithm is much suitable for practical application.

TABLE V
COMPARISON OF LOCALIZATION PERFORMANCE BETWEEN THE PROPOSED ALGORITHM AND FEATURE FUSION BASED ON THE MIDDLE LAYER AND BACK-END FUSION

	Acc	MAE	MSE	RMSE
feature fusion based on the middle layer	89.00%	0.545	2.111	1.453
back-end fusion	93.38%	0.292	1.155	1.075
the proposed algorithm	96.75%	0.263	1.005	1.002

V. CONCLUSION

In this article, a new CSI fingerprint and GCN based indoor localization algorithm is proposed by graph structure fusion. The amplitude and phase information are used for CSI gray image construction, respectively. The obtained amplitude and phase based CSI images are transformed into RGB image through rendering technique. Then, the CSI RGB image is proposed to form the corresponding graph structure of R, G and B channels. Finally, the front-end fusion is used to fuse all graph structures and obtain the final graph structure for GCN training.Experimental results show that the proposed algorithm has better localization performance than some existing methods.

REFERENCES

[1] Xiong H , Peng M , Gong S , et al. A Novel Hybrid RSS and TOA Positioning Algorithm for Multi-Objective Cooperative Wireless Sensor Networks[J]. IEEE Sensors Journal, 2018:1-1.

[2] Zhao K , Zhao T , Zheng Z , et al. Optimization of Time Synchronization and Algorithms with TDOA Based Indoor Positioning Technique for Internet of Things[J]. Sensors, 2020, 20(6513).

[3] Fokin G . AOA Measurement Processing for Positioning using Unmanned Aerial Vehicles[C]// 2019 IEEE International Black Sea Conference on Communications and Networking (BlackSeaCom). IEEE, 2019.

[4] Xue W , Hua X , Li Q , et al. A New Weighted Algorithm Based on the Uneven Spatial Resolution of RSSI for Indoor Localization[J]. IEEE Access, 2018, 6:26588-26595.

[5] Kipf T N , Welling M . Semi-Supervised Classification with Graph Convolutional Networks[J]. 2016.

[6] Wang X , Gao L , Mao S . BiLoc: Bi-modal Deep Learning for Indoor Localization with Commodity 5GHz WiFi[J]. IEEE Access, 2017, 5(99):4209-4220.

[7] Y. Xie, Z. Li and M. Li, "Precise Power Delay Profiling with Commodity Wi-Fi," in IEEE Transactions on Mobile Computing, vol. 18, no. 6, pp. 1342-1355, 1 June 2019.
[8] Dang X , Si X , Hao Z , et al. A Novel Passive Indoor Localization Method by Fusion CSI Amplitude and Phase Information[J]. Sensors, 2019, 19(4).
[9] Scarselli F , Tsoi A C , Gori M , et al. Graphical-Based Learning Environments for Pattern Recognition[C]// Structural, Syntactic, and Statistical Pattern Recognition, Joint IAPR International Workshops, SSPR 2004 and SPR 2004, Lisbon, Portugal, August 18-20, 2004 Proceedings. DBLP, 2004.
[10] Gori M , Monfardini G , Scarselli F . A new model for learning in graph domains[C]// IEEE International Joint Conference on Neural Networks. IEEE, 2005.
[11] Scarselli F , Gori M , Tsoi A C , et al. The graph neural network model[J]. IEEE Transactions on Neural Networks, 2009.
[12] Y. Fu, X. Xiong, Z. Liu, X. Chen, Y. Liu and Z. Fu, "A GNN-based indoor localization method using mobile RFID platform," 2022 7th International Conference on Smart and Sustainable Technologies (SpliTech), 2022, pp. 1-6.
[13] Sun Y , Xie Q , Pan G , et al. A Novel GCN based Indoor Localization System with Multiple Access Points[C]// 2021 International Wireless Communications and Mobile Computing (IWCMC). 2021.
[14] Lezama F, González G G, Larroca F, et al. Indoor Localization using Graph Neural Networks[C]//2021 IEEE URUCON. IEEE, 2021: 51-54.
[15] Yan W , Jin D , Lin Z , et al. Graph Neural Network for Large-Scale Network Localization[C]// International Conference on Acoustics, Speech, and Signal Processing. IEEE, 2020.
[16] Jung T W, Jeong C S, Kwon S C, et al. Point-Graph Neural Network Based Novel Visual Positioning System for Indoor Navigation[J]. Applied Sciences, 2021, 11(19): 9187.
[17] Chen B J , Chang R Y . Few-Shot Transfer Learning for Device-Free Fingerprinting Indoor Localization[J]. arXiv e-prints, 2022.
[18] Liu W , Cheng Q , Deng Z , et al. C-GCN: A Flexible CSI Phase Feature Extraction Network for Error Suppression in Indoor Positioning. 2021.